Egyptian Journal of Chemistry

Charge transfer complexes of atenolol drug with some dihydrxyanthraquinone and dihydroxybenzoquinone derivatives: Molecular structural, spectral, and quantitative studies.

Reem Mohammad Alghanmi[*]

[*]*University of Jeddah, College of Science, Department of Chemistry, Jeddah, Saudi Arabia*

Abstract

Atenolol (ATN) is β-blocker medication widely used in the clinic to treat hypertension. In this study, complexation of ATN with three different acceptors, namely alizarin (AZ), alizarin red S (AZR), and 2,5-dihydroxy-*p*-benzoquinone (DHBQ) was investigated spectrophotometrically. It was found that ATN formed charge transfer (CT) complexes with AZ, AZR, and DHBQ in MeOH. The CT reaction conditions between ATN and each acceptor were comprehensively investigated. Moreover, the formation constants and other related spectrophysical parameters were determined. The stoichiometry of 1:1 ratio was established for all studied complexes in MeOH using different methods. The optical band gap (E_g), which corresponds to the minimum energy required for the transition, was calculated by the optical absorption method. The values of E_g were found to be 2.02, 2.07, and 2.25 eV for the [ATN-AZ], [ATN-AZR], and [ATN-DHBQ] complexes, respectively. Solid complexes of ATN with these acceptors were effectively prepared and isolated. New bands in the FTIR spectra of the complexes were detected as a result of complexation. Additionally, the appearance of signals corresponding to the reactants in ^{1}H NMR spectra of the products confirmed the formation of ATN complexes. In addition to the CT reactions between ATN and each acceptor, both FTIR and ^{1}H NMR analyses suggested the existence of proton transfer reactions. Based on the fast complexation of ATN with the studied acceptors in MeOH, three direct, simple, and sensitive spectrophotometric methods were developed for the quantitative determination of ATN in its pure form and in pharmaceutical formulations. Validation studies confirmed the remarkable accuracy and precision of the developed methods without any interference from tablet excipients.

Keywords: Atenolol, Charge transfer, Validation, Alizarin, Proton transfer

Introduction

Cardiovascular diseases afflict a large number of people worldwide. Hypertension is the most common cardiovascular disorder, sometimes leading to stroke and other heart conditions. Numerous drugs for controlling hypertension have been developed, e.g., α-adrenergic antagonists, β-receptor antagonists, angiotensin-converting enzyme inhibitors, calcium channel blockers, and diuretics [1]. Atenolol (ATN), or 2-{4-[2-hydroxy-3-(propan-2-ylamino)propoxy] phenyl}acetamide, is an example of a β-blocker widely utilized for regulating the disease (Scheme 1). ATN does not exhibit membrane-stabilizing and intrinsic sympathomimetic effects [2,3]. It can be used alone or in combination with other agents to treat high blood pressure. It is also administered to prevent angina, migraines, and to improve survival following a heart attack [4]. Due to the extensive applications of ATN in the field of cardiology, and considering the risk associated with long-term use of the medicines, development of methods for the quantitative determination of ATN is essential.
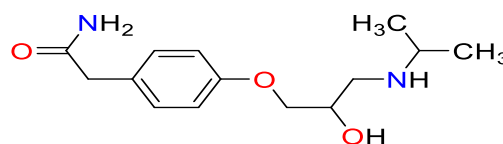
Scheme 1. Chemical structure of ATN drug.

The British Pharmacopoeia (1988) [5] as well as the United States Pharmacopoeia (2009) [6] described

_____

high-performance liquid chromatography (HPLC) as the official method for the detection of ATN. On the other hand, the Indian Pharmacopoeia (1996) [3], and the British Pharmacopoeia (2001) [7] recommended ultraviolet-visible (UV-vis) spectroscopy for the determination of ATN in tablets. In addition to these methods, several other analytical techniques were developed and reported for the assay of ATN in pure and dosage forms. These approaches include differential scanning calorimetry (DSC), thermogravimetric analysis (TGA) [8], electrophoresis [9-13], fluorometry [14, 15], Fourier-transform infrared (FTIR) spectroscopy [16], gas chromatography (GC) [17, 18], HPLC [19], high performance thin layer chromatography [20, 21], potentiometry [22-24], voltammetry [25, 26], and derivative spectrophotometry [27, 28]. However, the majority of these methods are associated with several disadvantages, such as lengthy measurements, necessity for heat or extraction steps, use of large amounts of expensive reagents, poor sensitivity, and requirement for complex apparatus.

In analytical chemistry, simple, fast, accurate, and sensitive spectrophotometric methods are highly desirable for routine drug analysis in control laboratories. Several visible spectrophotometric approaches have been reported for the determination of ATN in pharmaceutical formulations [4, 29-39]. Upon the formation of a charge transfer (CT) complex, an electronic charge is transferred from an electron donor molecule to an electron acceptor. Consequently, the donor becomes partially positively charged, whereas the acceptor exhibits a negative charge. Moreover, a weak electrostatic bond is formed between the molecules, resulting in the generation of an intensely colored product. A number of drugs are considered as good donors; therefore, it was speculated that effective spectrophotometric methods could be developed based on the rapid formation of CT complexes.

Alizarin (AZ) and alizarin red S (AZR), have been employed as electron acceptors for the spectrophotometric determination of various pharmaceutical compounds [40-48]. In addition, 2,5-dihydroxy-*p*-benzoquinone (DHBQ), an electron acceptor, was reported to form a colored CT complex with different amines [49, 50]. In the present study, these acceptors were shown to rapidly react with ATN at room temperature to form colored ion-pair complexes, which could be accurately detected by spectrophotometry. To the best of our knowledge, the current work is the first report on the use of AZ, AZR, as electron acceptors for the determination of ATN. Furthermore, DHBQ has not been previously

investigated as a chromogenic reagent for the detection of any drugs. Thus, we aimed to develop simple and rapid spectrophotometric methods for the quantitative determination of ATN in its pure form and in pharmaceutical formulations. The synthesis and characterization of the solid CT complexes consisting of ATN and each electron acceptor were essential to elucidate the nature of their interactions. Elemental analysis, electronic absorption spectrophotometry, FTIR, and ^{1}H NMR spectroscopy were used to characterize the obtained CT complexes.

Experimental
Materials and standard solutions
The chemicals used were of analytical grade and highest purity. ATN ($C_{14}H_{22}N_2O_4$) was obtained from Acros Organics. The acceptors, i.e., AZ, 1,2-dihydroxyanthraquinone ($C_{14}H_8O_4$), AZR, ($C_{14}H_8O_7S$), and DHBQ ($C_6H_4O_4$) were purchased from Sigma-Aldrich. HPLC grade methanol (MeOH) was obtained from Fisher Scientific. Stock solutions of ATN (5.0×10^{-3} mol L^{-1} and 200 μg mL^{-1}) were prepared in MeOH. Standard stock solutions of AZ and AZR (1.0×10^{-3} mol L^{-1}) and of DHBQ (5.0×10^{-3} mol L^{-1}) were also prepared in MeOH. All solutions were stored in a dark and cold place. The standards were stable for at least three days.

Apparatus
The electronic absorption spectra of ATN, AZ, AZR, DHBQ, and the formed CT complexes were measured over a wavelength range of 350−700 nm using a Shimadzu UV-1800 (Japan) spectrophotometer equipped with a quartz cell with a path length of 1.0 cm. The spectrophotometer was connected to a Shimadzu TCC-ZUOA temperature controller unit. The IR spectra of the solid CT complexes were recorded on Frontier spectrophotometer (PerkinElmer, USA). The ^{1}H NMR (700 MHz) spectra were obtained using a Bruker DPX spectrometer. The elemental analysis (CHN) was conducted with the Micro Analyzer 2400 (Perkin Elmer, USA).

Construction of calibration curve
Different volumes of the standard ATN solution were transferred to a series of 10-mL calibration flasks to obtain the final concentration ranges (1.00−160 μg mL^{-1}). Subsequently, 2 mL of 1.0×10^{-3} mol L^{-1} AZ or AZR solutions, or 1 mL of 5.0×10^{-3} mol L^{-1} DHBQ solution was added to each flask. The drug-acceptor mixture was then diluted with MeOH. The absorbance of all solutions was recorded at 528, 537, and 487 nm for AZ, AZR, and DHBQ, respectively,

_____

against acceptor blank. The absorbances of all solutions were plotted against ATN to construct the calibration curves.

Preparation of the pharmaceutical samples

The following pharmaceutical forms of ATN were obtained from the local pharmacy and subjected to analysis: Tenormin tablets (50 mg ATN per tablet) from AstraZenerca, UK, and Tensotin tablets (50 mg ABZ per tablet) from Julphar Gulf Pharmaceutical Industries, UAE. Ten tablets of each drug were weighed and ground to a powder. Accurately weighed portions of the powders equivalent to 50 mg of ATN was dissolved in 50 mL of MeOH. The solutions were then stirred for 30 min. Lastly; the solutions were filtered and diluted to 100 mL with MeOH to have a final concentration of 500 $\mu g\ mL^{-1}$. Aliquots from each solution were used for analysis employing the proposed methods.

Synthesis of the solid CT complex

Three solid CT complexes of ATN with AZ, AZR, and DHBQ were synthesized by dissolving 0.2 mmol of each reactant in 20 mL MeOH. The ATN solution was added to the solution of each acceptor and stirring for 3 h. The solvent was then evaporated at room temperature. The resulting solid products were collected, washed with MeOH, and stored in a desiccator for several days.

Results and discussion
Electronic absorption spectra

The electronic absorption spectra of ATN (5.0×10^{-4} mol L^{-1}), AZ (1.0×10^{-4} mol L^{-1}), AZR (1.0×10^{-4} mol L^{-1}), and DHBQ (5.0×10^{-4} mol L^{-1}), as well as those of the resulting CT complexes in MeOH were recorded in the region of 350−700 nm at 20 ± 2 °C (Figure 1). Notably, new absorption bands were detected in the spectra of the formed complexes in the regions, in which neither the donor nor the acceptors exhibited any bands. These CT bands were found at λ_{max} 533, 536, and 487 nm for [ATN-AZ], [ATN-AZR], and [ATN-DHBQ], respectively, and were attributed to the $\pi-\pi^*$ transitions. A noticeable change in the color of the solutions was observed upon mixing of ATN donor with each π-acceptor (i.e., AZ, AZR, or DHBQ) in MeOH. Importantly, the spectra of all CT complexes were measured against each acceptor as blank to eliminate a possible overlap between the complex and acceptor bands. It was previously reported that in polar solvents, CT reactions produce radical ions of the donor and acceptor. On the other hand, in non-polar solvents, outer sphere CT complexes, which include hydrogen bonding, are the major products [50]. Accordingly,

the intense color of the new CT complexes was a result of the formation of radical ions of the reactants as well as the total transfer of the charge from ATN to the acceptor. It is noteworthy that the absorbances of the CT complexes increased with increasing concentration of ATN, which confirms the stability of the formed complexes (Figure 2).
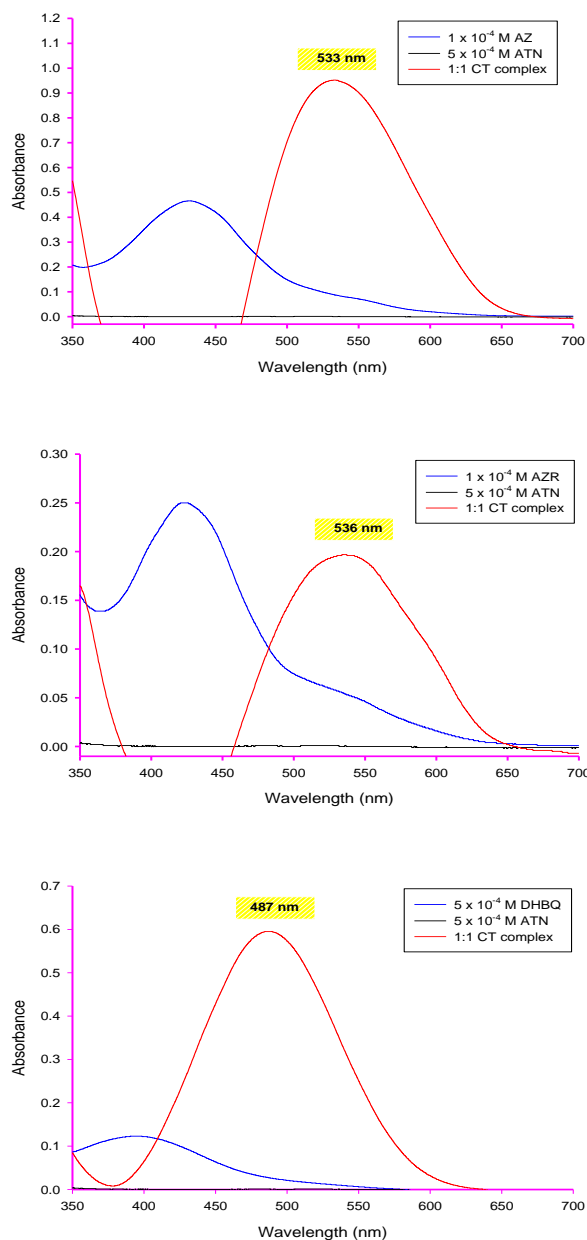

Figure 1. Electronic absorption spectra of ATN complexes with AZ, AZR, and DHBQ in MeOH at 20 ± 2 °C.
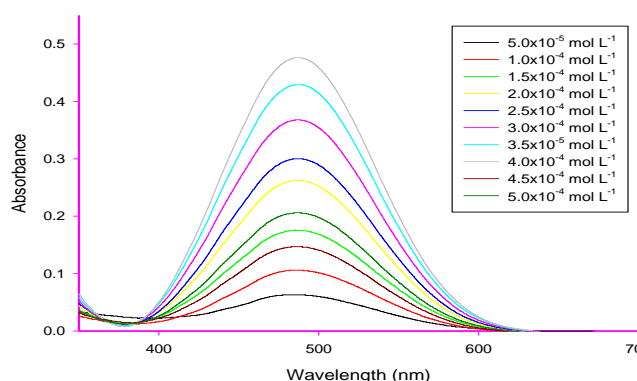
Figure 2. Electronic absorption spectra of [ATN-DBQ] complex in MeOH.

Optimization of the CT reaction conditions

We subsequently investigated the optimum conditions affecting the stability of the formed CT complexes. Each condition was individually changed while keeping the others constant. The optimum reaction time was evaluated by measuring the absorbance of the CT complexes at room temperature (20 ± 2 °C). The highest absorbance was detected immediately after adding the acceptor solution (AZ, AZR, or DHBQ). Moreover, no increase in the complex absorbance was observed with the increase of the reaction time (Figure 3). Thus, the absorbance was recorded immediately after mixing ATN with each acceptor. Furthermore, the optimal temperature was tested by recording the absorbance of the CT complexes over the temperature range of 20 °C to 45 (Figure 4). It is evident from Figure 4 that the absorbances of [ATN-AZ] and [ATN-AZ] decreased with increasing temperature, while the absorbance of [ATN-DHBQ] was constant over the studied temperatures. Hence, 20 °C (293 K) was the optimal temperature for all ATN complexes.
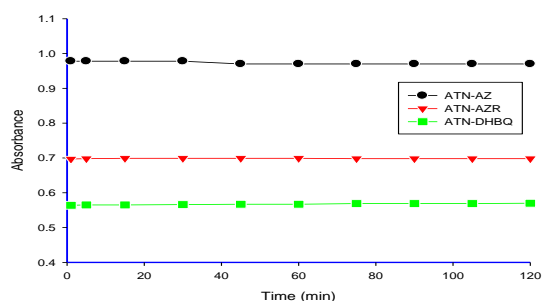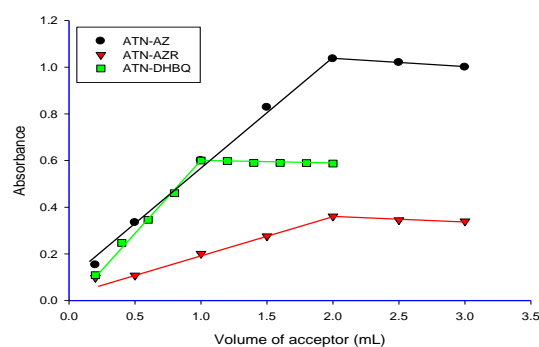

Figure 3. Effect of time on the absorbance of ATN complexes in MeOH at 20 ± 2 °C.
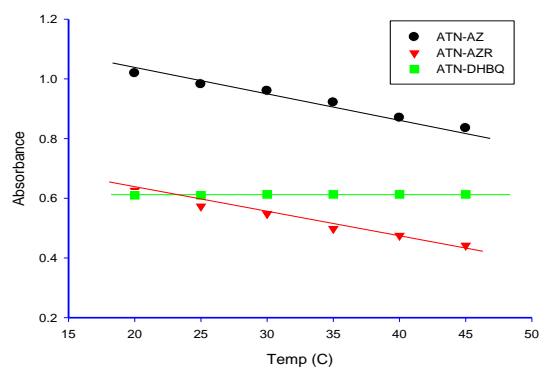
Figure 4. Effect of temperature on the absorbance of ATN complexes in MeOH.

ATN and the studied acceptors exhibited limited solubility in non-polar solvents. Therefore, the CT reaction of the drug with different acceptors was investigated just in polar-solvents, such as ethanol (EtOH), MeOH, and acetonitrile (MeCN). Table 1 demonstrates the spectral characterization data for ATN complexes formed in the above solvents. Utilizing MeOH resulted in the formation of complex with the highest color intensity; thus, this solvent was selected for all CT reactions. We then also evaluated suitable acceptor concentration. It was found that using 2.0 mL of 1.0×10^{-3} mol L^{-1} AZ or AZR solutions, or 1.0 mL of a 5.0×10^{-3} mol L^{-1} DHBQ solution afforded the maximum stable absorbance (Figure 5).

Figure 5. Effect of acceptor concentration on the absorbance of ATN complexes in MeOH at 20 ± 2 °C.

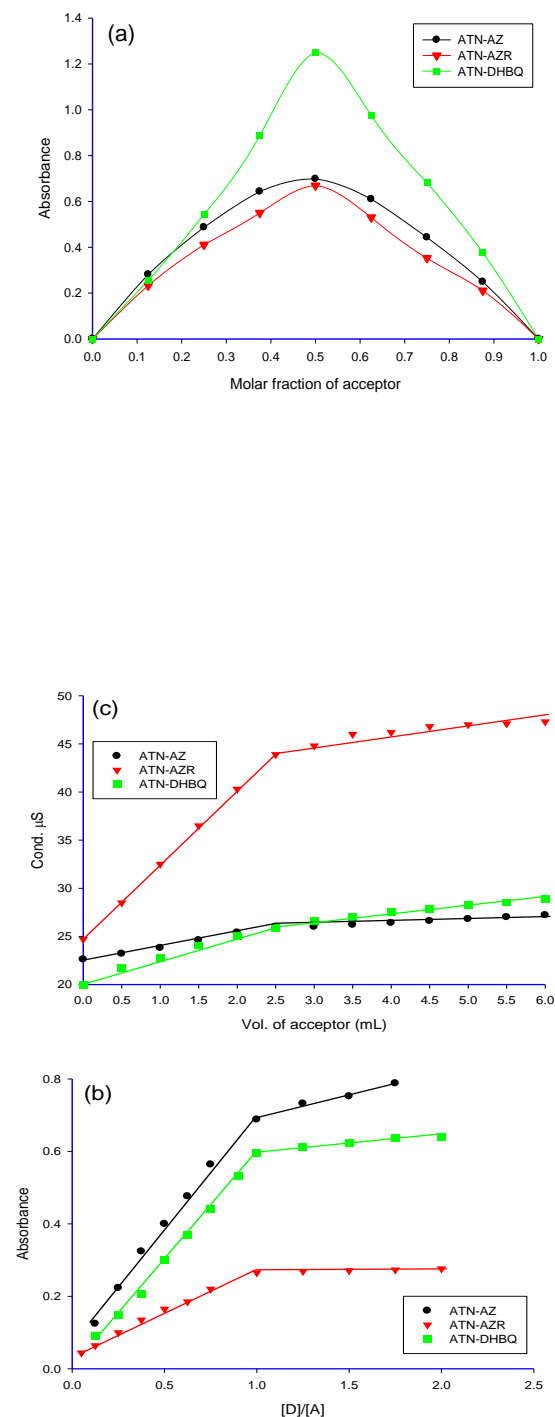**Table 1. Effect of solvent on the spectral characterization of the ATN complexes.**

Acceptor	Solvent	ATN Conc. (mol L^{-1})	Absorbance	ε (L mol^{-1} cm^{-1})
AZ	EtOH	5.0×10^{-4}	0.387	774
	MeOH	5.0×10^{-4}	0.952	1904
	MeCN	5.0×10^{-4}	0.157	314
AZR	EtOH	5.0×10^{-4}	0.222	444
	MeOH	5.0×10^{-4}	0.350	700
	MeCN	5.0×10^{-4}	0.150	304
DHBQ	EtOH	5.0×10^{-4}	0.579	1158
	MeOH	5.0×10^{-4}	0.595	1190
	MeCN	5.0×10^{-4}	0.265	530

plots. Based on this data, the strongest interaction between ATN and the π-acceptors occurred at a 1:1 ratio (Figure 6).

Stoichiometry of the CT reaction

The stoichiometry of the complexes of ATN with AZ, AZR, or DHBQ in MeOH was estimated employing Job's method of continuous variation [51], spectrophotometric titration, and conductometric titration. The Job's method was performed using equimolar concentrations of the drug and each acceptor (1.0×10^{-3} and 1.0×10^{-4} mol L^{-1} for reactions with AZ, AZR, and DHBQ, respectively). Spectrophotometric titration was conducted by recording the absorbances of the CT complexes at different molar ratios. Furthermore, for conductometric titrations, 25 mL of a 1.0×10^{-4} mol L^{-1} of ATN solution was titrated with 1.0×10^{-3} mol L^{-1} solution of each acceptor at 20 °C using a conductivity cell exhibiting a cell constant (K) of 0.96 cm^{-1}. Subsequently, the conductivity was recorded after each addition of the acceptor solution at 2 min intervals. The stoichiometry was determined by plotting the volume of the acceptor against the recorded conductivity.

The plots obtained for each approach are demonstrated in Figure 6 (a, b, and c for Job's method, photometric titration, and conductometric titration, respectively). The Job's plot reached the highest value at a mole fraction of 0.5 for complexation of ATN with AZ, AZR, or DHBQ, indicating a molar reaction ratio of 1:1 between the drug and acceptors. A similar observation was made for both photometric and conductometric titration

Figure 6. The stoichiometric ratio of the interaction between ATN and AZ, AZR, or DHBQ using: (a) Job's method, (b) photometric titration, and (c) conductometric titration, in MeOH at 20 ± 2 °C.

Determination of the formation constant and molar extinction coefficient

The stability of the new ATN complexes was estimated by calculating the formation constant, K_{CT} (L mol^{-1}), and the molar extinction coefficient, ε (L mol^{-1} cm^{-1}). Benesi-Hildebrand equation [52] was used to calculate K_{CT} and ε by measuring the absorbance of the ATN complexes formed by the additions of different concentrations of the drug to a certain concentration of each acceptor as follows:

$$\frac{C_A}{Abs} = \frac{1}{K_{CT}\varepsilon} \cdot \frac{1}{C_D} + \frac{1}{\varepsilon} \qquad (1)$$

In the above equation, C_A and C_D indicate the initial concentrations of the acceptor and ATN, respectively, while *Abs* is the absorbance of the CT complex at λ_{max}. Straight lines were obtained when C_A/Abs was plotted against $1/C_D$, and the correlation coefficient (r ≥ 0.9875), confirmed the formation of 1:1 CT complexes (Figure 7). The K_{CT} and ε values for all ATN complexes are summarized in Table 2. All ATN complexes recorded high K_{CT} and ε values, which demonstrated the high stability of the CT complexes in MeOH. Notably, the [ATN-AZR] complex displayed the highest K_{CT} and the lowest ε, whereas the lowest value of K_{CT} and the highest value of ε were recorded for [ATN-DHBQ] complex.
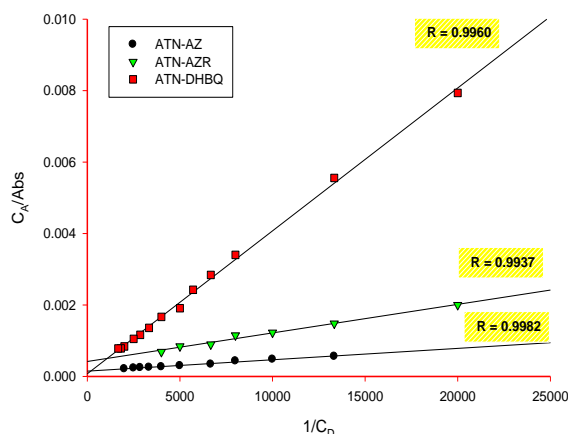

Figure 7. Benesi-Hildebrand plots for the ATN CT complexes in MeOH

Determination of the spectroscopic parameters

The spectroscopic parameters, including the CT energy, E_{CT} (eV), the ionization potential of the donor (i.e., ATN), I_D (eV), the oscillator strength, *f*, transition dipole moment, μ (debye), the resonance energy, R_N (eV), and the standard free energy change, $\Delta G°$ (kJ mol^{-1}), were calculated for all ATN complexes according to a previously described methods [53-59]. The following equations were used to obtain the desired parameters:

$$E_{CT} = \frac{1243.667}{\lambda_{CT}(nm)} \qquad (2)$$

$$I_D = 5.76 + 1.53 \times 10^{-4} \cdot \nu_{CT} \qquad (3)$$

$$f = 4.319 \times 10^{-9}\left[\varepsilon_{CT} \cdot \Delta\nu_{1/2}\right] \qquad (4)$$

$$\mu = 0.0958\left[\varepsilon_{CT} \cdot \Delta\nu_{1/2} / \overline{\nu}_{CT}\right]^{1/2} \qquad (5)$$

$$\varepsilon_{CT} = 7.7 \times 10^4 / [h\nu_{CT} / [R_N] - 3.5] \qquad (6)$$

$$\Delta G^o = -2.303RT \log K_{CT} \qquad (7)$$

Table 2. Spectal data of ATN complexes with different acceptors in MeOH.

Acceptor	C^o_A (mol L^{-1})	C^o_D (mol L^{-1})	Absorbance	K_{CT} (L mol^{-1})	ε (L mol^{-1} cm^{-1})	R^2
	At 293 K		at $\lambda_{CT\,(533\,nm)}$			
	2.0×10^{-4}	2.5×10^{-5}	0.124	2.50×10^3	10.0×10^3	0.9964
	2.0×10^{-4}	5.0×10^{-5}	0.223			
	2.0×10^{-4}	7.5×10^{-5}	0.357			
	2.0×10^{-4}	1.0×10^{-4}	0.418			
	2.0×10^{-4}	1.3×10^{-4}	0.466			
AZ	2.0×10^{-4}	1.5×10^{-4}	0.588			
	2.0×10^{-4}	2.0×10^{-4}	0.673			
	2.0×10^{-4}	2.5×10^{-4}	0.753			
	2.0×10^{-4}	3.0×10^{-4}	0.788			
	2.0×10^{-4}	3.5×10^{-4}	0.817			
	2.0×10^{-4}	4.0×10^{-4}	0.862			

	2.0×10^{-4}	5.0×10^{-4}	0.952			
	At 293 K		at $\lambda_{CT\ (536\ nm)}$			
	2.0×10^{-4}	5.0×10^{-5}	0.100	5.00×10^3	2.50×10^3	0.9875
	2.0×10^{-4}	7.5×10^{-5}	0.135			
	2.0×10^{-4}	1.0×10^{-4}	0.163			
AZR	2.0×10^{-4}	1.3×10^{-4}	0.174			
	2.0×10^{-4}	1.5×10^{-4}	0.223			
	2.0×10^{-4}	2.0×10^{-4}	0.237			
	2.0×10^{-4}	2.5×10^{-4}	0.291			
	At 293 K		at $\lambda_{CT\ (487\ nm)}$			
	5.0×10^{-4}	7.5×10^{-5}	0.090	2.70×10^2	12.00×10^3	0.9920
	5.0×10^{-4}	1.0×10^{-4}	0.106			
	5.0×10^{-4}	1.3×10^{-4}	0.147			
	5.0×10^{-4}	1.5×10^{-4}	0.176			
	5.0×10^{-4}	1.8×10^{-4}	0.206			
DHBQ	5.0×10^{-4}	2.0×10^{-4}	0.262			
	5.0×10^{-4}	2.5×10^{-4}	0.300			
	5.0×10^{-4}	3.0×10^{-4}	0.368			
	5.0×10^{-4}	3.5×10^{-4}	0.429			
	5.0×10^{-4}	4.0×10^{-4}	0.476			
	5.0×10^{-4}	5.0×10^{-4}	0.595			
	5.0×10^{-4}	5.5×10^{-4}	0.637			

Table 3. The spectroscopic physical parameters of the ATN complexes in MeOH.

Complex	λ_{CT} (nm)	E_{CT} (eV)	I_D (eV)	f	μ (Debye)	R_N (eV)	$-\Delta G°$ (kJ mol^{-1})
[ATN-AZ]	533	2.33	8.63	1.35	12.4	5.31	19.40
[ATN-AZR]	536	2.32	8.61	0.80	9.53	3.33	21.12
[ATN-DHBQ]	487	2.55	8.90	0.91	9.70	3.77	13.22

The values of the calculated spectroscopic parameters are presented in Table 3. The E_{CT} values in Table 3 were low and differed between the three ATN complexes, indicating that the CT transition in these complexes depended on the nature of the acceptors. The I_D values were also relatively low and consistent with the high values of K_{CT}. It is noteworthy that the I_D value reflects the donating power of the donor (ATN). The donating power of ATN and the stability of the complexes increased with decreasing I_D value. The high stability of the [ATN-AZR] complex was a result of strong interactions between the ATN and acceptor radical ions [60].

All studied complexes exhibited high f, μ, and R_N parameter values, indicating the presence of strong CT interactions between the ATN and each acceptor. The parameters were the highest for the [ATN-AZR] complex, and the lowest values for the [ATN-DHBQ] complex. As shown in Figure 8, the value of f strongly correlates with μ (R = 0.9906) and R_N (R = 0.998). On the other hand, there was no correlation between f and K_{CT} or ε_{CT}. Finally, negative $\Delta G°$ values were obtained for all ATN complexes (Table 3), suggesting that the reaction between ATN and the corresponding acceptors was spontaneous. The $\Delta G°$ value became more negative in the same order as the K_{CT} value of all ATN complexes.
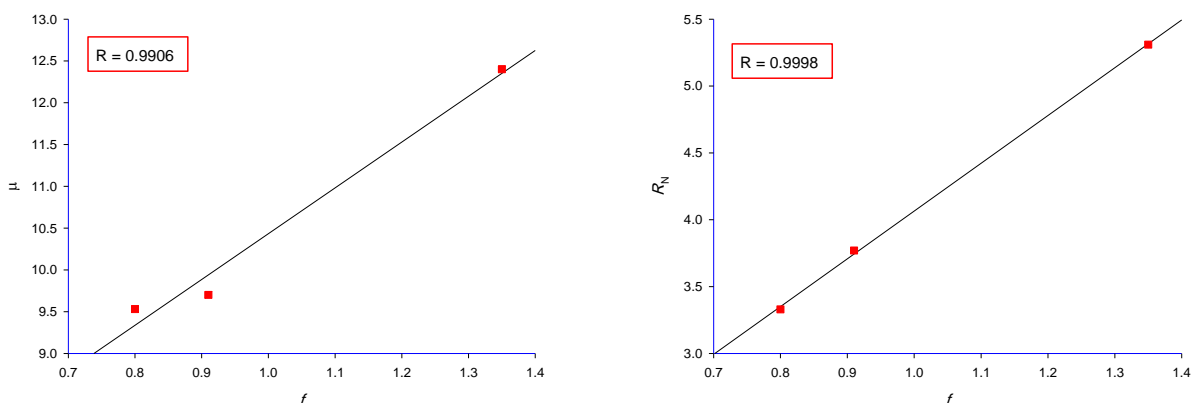
Figure 8. Linear correlations of the oscillator strength (*f*) with the transition dipole moment (*μ*), and the resonance energy (*R*$_N$).

Determination of the optical band gap *E*$_g$

The energy difference between the top of the valence band and the bottom of the conduction band is called the "band-gap." The band-gap energy (*E*$_g$) is the minimum amount of energy required by an electron to transfer from the valence band to the conduction band [61]. In an absorption process, an electron is excited from a lower to a higher energy level, i.e., the absorption edge, by absorbing a photon with a specific energy. The optical absorption near the absorption band edge can be used to estimate *E*$_g$ and confirm the formation of CT complex. The absorption coefficient (α) can be determined from the transmittance *T* of the complex, according to the following equation expresses it:

$$\alpha = \frac{1}{d} lin\left(\frac{1}{T}\right) \tag{8}$$

where *d* is the thickness of the sample. On the other hand, the band-gap of CT complex can be determined from the relationship between α and *E*$_g$ according to the following equation [62]:

$$\alpha h\nu = A(h\nu - E_g)^m \tag{9}$$

where *m* equals to ½ and 2 for direct and indirect transition, respectively, whereas *A* indicates an energy-independent constant. As demonstrated in Figure 9, for each complex, the values of (α*h*ν)^2 were plotted against *h*ν. The direct optical band-gap *E*$_g$ was determined from the linear sections of the plots at the absorption edge where (α*h*ν)^2 = 0 [61], and its values were found to be 2.02, 2.07, and 2.25 eV for [ATN-AZR], [ATN-AZ], and [ATN-DHBQ],

respectively. These values indicate the semiconducting behavior of the new ATN complexes [63, 64]. Moreover, the dependence of *E*$_g$ value on the nature of the acceptor was evidenced by the difference in the obtained values.

Validation of the methods

Based on the formation of stable colored complexes of ATN with AZ, AZR, or DHBQ, three spectrophotometric methods were developed to determine the concentration of the drug in the pure and in pharmaceutical dosage. The linearity, accuracy, precision, robustness, sensitivity, and recovery of the proposed methods were evaluated according to the International Conference on Harmonization (ICH) guidelines [65]. Linearity, regression equations, and sensitivity parameters of the methods are summarized in Table 4. The methods were found to be linear over the ranges of 1.0−150, 1.0−80, and 1.0−150 μg mL^{-1} for AZ, AZR, DHBQ acceptors, respectively, with excellent correlation coefficient values (*R* ≥ 0.994). In addition, the *LOD* and *LOQ* values listed in Table 4 were small, which indicated the sensitivity of the developed methods. Intra-day and inter-day analyses were conducted to determine the accuracy and precision of the methods, and the results of the evaluation are shown in Table 5. The values of recovery percentage, %RSD, and %RE in Table 5 suggested the high repeatability and reproducibility of the methods. The robustness of the methods was examined by investigating the influence of small variations in the variables, such as reagent volume (± 0.1 mL) and time (± 0.50 min). The obtained data are demonstrated in Table 6. The results showed that during the determination of ATN,

the proposed methods were not significantly affected by the variations in the variables.

The methods were further validated by performing a recovery study. Three different concentration levels (50%, 100%, and 150%) of the standard pure ATN solution were added to the sample solution of the pharmaceutical drug (Tenormin® and Tensotin® tablets). The total concentration was determined using the methods. The recovery percentages in Table 7 were ranged from 99.20 % to 101.1 % for all three acceptors, with %RSD values of < 1.47 %. These outcomes confirmed that the co-formulated materials and common ingredients did not interfere with the ATN assay.
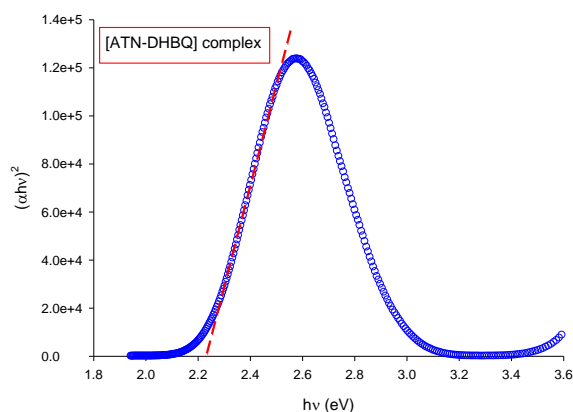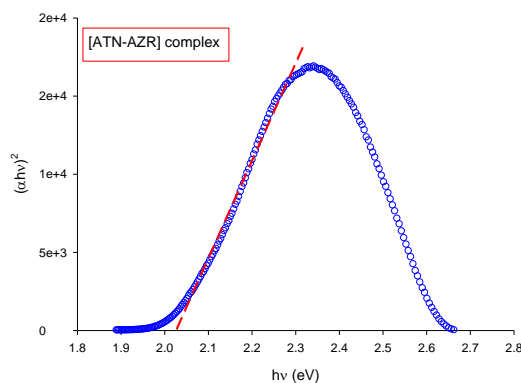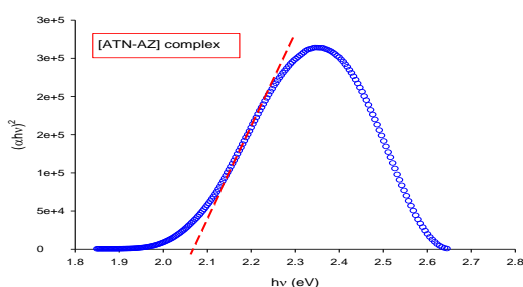

Figure 9. Plots of photon energy (hν) against (αhν)² for the ATN complexes in MeOH.

Table 4. Linearity, regression equation and sensitivity parameters of the proposed methods ($n = 7$).

Parameter	Acceptor		
	AZ	AZR	DHBQ
Conc. of acceptor, mol L^{-1}	1×10^{-3}	1×10^{-3}	5×10^{-3}
Volume of acceptor, mL	2	2	1
Temperature	20±2 °C	20±2 °C	20±2 °C
Reaction time, min	1	1	1
Wavelength (λ_{max}), nm	533	536	487
Linear range, µg mL^{-1}	1.00-150	1.00-80.8	1.00-150
Molar absorptivity (ε), L mol^{-1} cm^{-1}	501	872	1186
Limit of detection (LOD), µg ml^{-1}	1.078	1.641	1.343
Limit of quantification (LOQ), µg ml^{-1}	3.592	4.973	4.007
Regression equation^a			
Intercept, $a \pm S_a$	0.0001±9.76×10^{-4}	0.028±1.628×10^{-3}	0.0075±1.81×10^{-3}
Slope, $b \pm S_b$	0.0019±6.76×10^{-6}	0.033±0.037×10^{-3}	0.0045±2.54×10^{-5}
$S_{y/x}$	1.63 ×10^{-3}	2.95 ×10^{-3}	4.34 ×10^{-3}
Correlation coefficient, R	0.9998	0.9994	0.9997
Stability of colored product (h)	2	2	2

^{a} $A = a + bC$, where A is the absorbance, C is the ATN concentration in (µg ml^{-1}), a is the intercept and b is the slope.

Application of the proposed methods

The developed methods were utilized to determine the concentration of ATN in the Tenormin® and Tensotin® tablets. Tables 8 and 9 demonstrated the results of the analyses for the Tenormin® and Tensotin® tablets as ATN concentration ± standard deviation, respectively. Statistical comparison of the results obtained by three developed methods and those of the reference method [3] was carried out using F-test and student's t-test. The calculated F and t values were lower than the tablet values of F and student's t-test at 95 % confidence level which implied that there was no

significant difference between the proposed and reference methods.

Characterization of the solid CT complexes

A saturated solution of ATN was reacted with each of the three acceptors in MeOH, forming intensely colored solid products. These complexes were characterized by elemental analysis, FTIR spectroscopy, and ^{1}H NMR spectroscopy to confirm the complexation and to locate the position of the interaction between ATN and the acceptors. The donor: acceptor molar ratio for the complexes was 1:1 based on the elemental analysis results illustrated in Table 10

Table 5: Evaluation of intra-day and inter-day accuracy and precision.

Acceptor	ATN taken, µg mL^{-1}	Intra-day ($n = 5$) Found, µg mL^{-1} ±Confidence limits[a]	%Recovery	%RSD[b]	%RE[c]	Inter-day ($n = 3$) Found, µg mL^{-1} ±Confidence limits[a]	%Recovery	%RSD[a]	%RE[b]
AZ	60	29.82 ± 0.62	99.39	1.67	0.61	29.45 ± 0.78	98.18	1.07	1.82
	80	49.64 ± 0.62	99.27	1.00	0.73	49.27 ± 2.26	98.55	1.85	1.45
	100	69.64 ± 0.62	99.48	0.72	0.52	69.58 ± 3.45	99.39	2.00	1.61
	120	89.10 ± 1.24	98.99	1.12	1.01	89.58 ± 3.45	99.53	1.55	0.47
AZR	8	7.982 ± 0.03	99.77	0.34	0.22	8.060 ± 0.07	100.8	0.34	0.79
	15	15.05 ± 0.05	100.3	0.24	0.31	15.09 ± 0.10	100.6	0.26	0.62
	18	17.97 ± 0.11	99.85	0.48	0.15	18.20 ± 0.21	101.1	0.47	1.10
	25	25.08 ± 0.06	100.3	0.20	0.32	25.09 ± 0.10	100.4	0.16	0.37
DHBQ	45	5.95 ± 0.02	99.17	0.34	0.83	5.94 ± 0.12	99.02	0.77	0.98
	65	7.97 ± 0.04	99.61	0.52	0.87	7.91 ± 0.24	99.64	1.18	0.36
	85	11.88 ± 0.08	98.98	0.64	1.02	11.93 ± 0.24	99.38	0.79	0.62
	105	16.82 ± 0.17	98.95	0.95	1.04	16.96 ± 0.28	99.74	0.67	0.26

[a] Average $\pm \dfrac{t_{0.05}SD}{\sqrt{n}}$, at 95% confidence level, [b] %RSD, relative standard deviation; [c] %RE, relative error.

.

Table 6: Robustness of the proposed methods.

Acceptor	Parameter	ATN taken, µg mL^{-1}	Found, µg mL^{-1} ±SD	%Recovery	%RSD
AZ (n = 5)	Volume of 5×10^{-4} mol L^{-1} AZ (2.0 ± 0.1 mL)	60	59.48 ± 0.40	99.14	0.67
		80	79.27 ± 0.83	99.09	1.05
		100	100.4 ± 0.70	100.4	0.69
		120	119.2 ± 0.66	99.31	0.55
	Reaction time (1.00 ± 0.50 min)	60	59.11 ± 0.29	98.51	0.48
		80	79.21 ± 0.80	99.01	1.01
		100	100.4 ± 0.79	100.8	0.47
		120	119.1 ± 0.60	99.25	0.50
AZR (n = 5)	Volume of 5×10^{-4} mol L^{-1} AZR (2.0 ± 0.1 mL)	30	29.79 ± 0.40	99.29	1.33
		50	50.03 ± 0.34	100.0	0.68
		70	70.33 ± 0.82	100.5	1.16
	Reaction time (1.00 ± 0.50 min)	30	30.21 ± 0.25	100.7	0.84
		50	49.94 ± 0.54	99.88	1.08
		70	70.48 ± 0.68	100.7	0.97
DHBQ (n = 5)	Volume of 1×10^{-4} mol L^{-1} DHBQ (1.0 ± 0.1 mL)	45	44.98 ± 0.27	99.95	0.61
		65	65.42 ± 0.29	100.4	0.44
		85	85.48 ± 0.18	100.6	0.22
		105	105.6 ± 0.42	100.6	0.39
	Reaction time (1.00 ± 0.50 min)	45	45.29 ± 0.25	100.6	0.56
		65	65.56 ± 0.25	100.8	0.39
		85	84.90 ± 0.47	99.88	0.56
		105	105.9 ± 0.36	100.9	0.34

Table 7: Results of recovery study for Tenormin® and Tensotin® tablets.

Tablet	Acceptor	ATN in tablet, µg mL^{-1}	Pure ATN added, µg mL^{-1}	Total found, µg mL^{-1} ± SD	%Recovery	%RSD
Tenormin	AZ (n = 5)	40.00	20.00	60.16 ± 0.88	100.3	1.46
		40.00	40.00	80.58 ± 0.94	100.7	1.17
		40.00	60.00	100.3 ± 0.96	100.3	0.95
	AZR (n = 5)	20.00	10.00	30.21 ± 0.25	100.7	0.84
		20.00	20.00	40.09 ± 0.54	100.2	1.35
		20.00	30.00	49.70 ± 0.34	99.39	0.68
	DHBQ (n = 5)	40.00	20.00	59.60 ± 0.29	99.33	0.49
		40.00	40.00	80.09 ± 0.35	100.1	0.44
		40.00	40.00	99.20 ± 0.52	99.20	0.52
Tensotin	AZ (n = 5)	40.00	20.00	59.94 ± 0.83	99.91	1.39
		40.00	40.00	80.58 ± 0.91	100.7	1.07
		40.00	60.00	101.1 ± 0.86	101.1	0.86
	AZR (n = 5)	20.00	10.00	29.85 ± 0.37	99.49	1.24
		20.00	20.00	39.79 ± 0.33	99.47	0.84
		20.00	30.00	50.06 ± 0.30	100.1	0.59
	DHBQ (n = 5)	40.00	20.00	59.73 ± 0.34	99.56	0.56
		40.00	40.00	80.10 ± 0.35	100.1	0.44
		40.00	60.00	100.5 ± 0.65	100.5	0.64

Table 8: Determination of ATN in Tenormin® tablets using AZ, AZR, and DHBQ accceptors.

Acceptor	ATN in tablet [taken], µg mL^{-1}	Found*, µg mL^{-1} ± SD		%Recovery		F-test	t-test
		Proposed method	Reference method [3]	Proposed method	Reference method [3]		
AZ	60	59.63 ± 0.71	58.89 ± 0.64	99.38	98.16	1.200	0.785
AZR	50	49.88 ± 0.27	49.48 ± 0.50	99.76	98.97	3.375	1.014
DHBQ	60	60.22 ± 0.60	60.40 ± 0.78	100.4	100.7	1.685	0.174

*Average value of five determinations.
The value of *t* (tabulated) at 95% confidence level is 2.306.
The value of *F* (tabulated) at 95% confidence level and is 6.388.

Table 9: Determination of ATN in Tensotin® tablets using AZ, AZR, and DHBQ accceptors.

Acceptor	ATN in tablet [taken], µg mL^{-1}	Found*, µg mL^{-1} ± SD		%Recovery		F-test	t-test
		Proposed method	Reference method [3]	Proposed method	Reference method [3]		
AZ	60	59.42 ± 0.91	58.89 ± 0.64	99.04	98.16	2.000	1.879
AZR	50	49.89 ± 0.27	49.63 ± 0.50	99.75	99.27	3.375	1.014
DHBQ	60	60.44 ± 0.62	60.71 ± 0.67	100.7	101.2	1.179	0.297

*Average value of five determinations.
The value of *t* (tabulated) at 95% confidence level is 2.306.
The value of *F* (tabulated) at 95% confidence level and is 6.388.

Table 10. Elemental analysis data of the synthesized complexes.

Complex	Molecular formula	M.wt g mol^{-1}	Elemental analysis						Molar ratio
			C%		H%		N%		
			Found	Calc.	Found	Calc.	Found	Calc.	
ATN-free	$C_{14}H_{22}N_2O_4$	266.34	62.91	63.13	8.26	8.33	10.31	10.52	–
ATN-AZ	$C_{28}H_{30}N_2O_7$	506.55	66.22	66.39	5.88	5.97	5.34	5.53	1:1
ATN-AZR	$C_{28}H_{30}N_2O_{10}S$	586.61	57.42	57.33	5.07	5.15	4.65	4.78	1:1
ATN-DHBQ	$C_{20}H_{26}N_2O_7$	406.43	59.17	59.10	6.32	6.45	6.77	6.89	1:1

FTIR spectra

The FTIR spectra of ATN, as well as the three solid complexes, were measured using a KBr disk in the region of 4000–400 cm^{-1} (Figure 10). It is noteworthy that in the solid-state, the ATN drug exhibited two intramolecular H-bonds. The first one was between the NH$_2$ and C=O moieties, while the second was between the NH and OH groups [66]. Thus, the FTIR spectrum of free ATN displayed two characteristic bands at 3350 and 3162 cm^{-1}, which corresponded to the stretching vibration of −OH, −NH$_2$, and −NH groups [67, 68]. In spectra of the complexes (Figure 10), the main IR bands of ATN and those of the studied acceptors shifted to lower or higher wavenumbers compared with those of free reactants. In addition, the intensities of the bands also changed, which confirming complexation between the ATN and the acceptors.

The FTIR spectrum of the [ATN-AZ] complex shows a change in the intensity of the stretching vibration bands of ATN at 3350 and 3162 cm^{-1}. Those bands became weaker and shifted to 3353 and 3170 cm^{-1}, respectively, in the complex spectrum. An important observation in the spectrum of [ATN-AZ] was also the disappearance of the ν(−OH) band ascribed to the AZ acceptor [69]. Moreover, a redshift of ν(−NH) band from 3162 cm^{-1} in the spectrum of ATN to 3170 cm^{-1} in the spectrum of the complex was noted. These results confirmed the migration of a proton from the OH moiety of AZ to the amide group of ATN. The ν_{as} and ν_{s} bands corresponded to the CH$_3$ groups of free ATN at 2964 and 2924 cm^{-1}, respectively, shifted to higher wavenumbers (i.e., 2967 and 2937 cm^{-1}). Furthermore, the ν(−CH$_2$) band at 2866 cm^{-1} shifted to a lower wavenumber of ~ 2700 cm^{-1}. The band also appeared weaker and broader in the complexes spectrum. These changes could be explained by the occurrence of proton transfer from AZ to ATN. Another important observation in the spectrum of [ATN-AZ] was the appearance of the ν(C=O) bands, which were ascribed to the anthraquinone moiety as a small shoulder at 1661 cm^{-1} and medium band at

1634 cm^{-1}. In contrast, two strong bands at 1669 and 1634 cm^{-1} were detected for ν(C=O) in the spectrum of AZ alone [70]. These outcomes suggested the involvement of one carbonyl group of AZ in an H-bond with the OH group in ATN. Additionally, the δ(−OH) band of free ATN (1300 cm^{-1}) was blue-shifted in the spectrum of the complex (1281 cm^{-1}), which could be explained by the formation of a H-bond between the OH group of ATN and the carbonyl functionality of AZ.

Significant changes in the ATN stretching bands at 3350 and 3162 cm^{-1} were observed in the spectrum of the [ATN-AZR] complex. The first band was split into two and became weaker, whereas the second sifted to 3217 cm^{-1}. On the other hand, the ν(−OH) band of AZR at 3460 cm^{-1} [70] was not visible in the spectrum of the [ATN-AZR] complex. These changes indicated a proton migration from the hydroxyl group of AZR to the NH moiety of ATN. Moreover, a change in the strong ν(C=O) bands of AZR at 1666 and 1634 cm^{-1} [75] were noted in the spectrum of the [ATN-AZR] complex. The first band appeared as a very weak shoulder, while the second became medium in intensity. Thus, the formation of a H-bond between the carbonyl group of AZR and the OH group of ATN was expected. Furthermore, the δ(−OH) band of ATN shifted from 1300 to 1266 cm^{-1} in the spectrum of [ATN-AZR], confirming the presence of H-bonding between ATN and AZR.

As shown in Figure 10, the spectrum of [ATN-DHBQ] complex exhibited a noticeable change in the stretching vibrations region between 3400 and 2500 cm^{-1} compared with the spectra of [ATN-AZ] and [ATN-AZR] complexes. The sharp stretching vibration band corresponding to both hydroxyl and amino moieties of free ATN shifted to lower wavenumber (3306 cm^{-1}) compared with that of free ATN (3350 cm^{-1}). In addition, a new stretching vibration band was observed in the spectrum of [ATN-DHBQ] at 3156 cm^{-1} instead of the stretching vibration bands corresponding to the amide and methyl groups at 3162, 2964, and 2924 cm^{-1} in the ATN spectrum. The new band was attributed to the proton transfer from the OH group of

DHBQ to the amide nitrogen of ATN, leading to the reduction of the amino and methyl vibrational bands [71]. Another band in the spectrum of the complex was detected at 2678 cm^{-1} and was ascribed to aliphatic $\nu(CH_2)$ and $\nu(CH)$ of the ATN. Moreover, the spectrum of [ATN-DHBQ] also exhibited a strong band at 1488 cm^{-1}, which corresponded to the overlap between $\delta(OH)$ and $\nu(C=C)$ of DHBQ. The shift of the $\nu(C=O)$ band of DHBQ from 1710 to 1688 cm^{-1} in the spectrum of the complex is also noteworthy (Figure 10). It was a result of the H-bonding interaction between the carbonyl group of DHBQ and the aliphatic OH moiety of ATN.
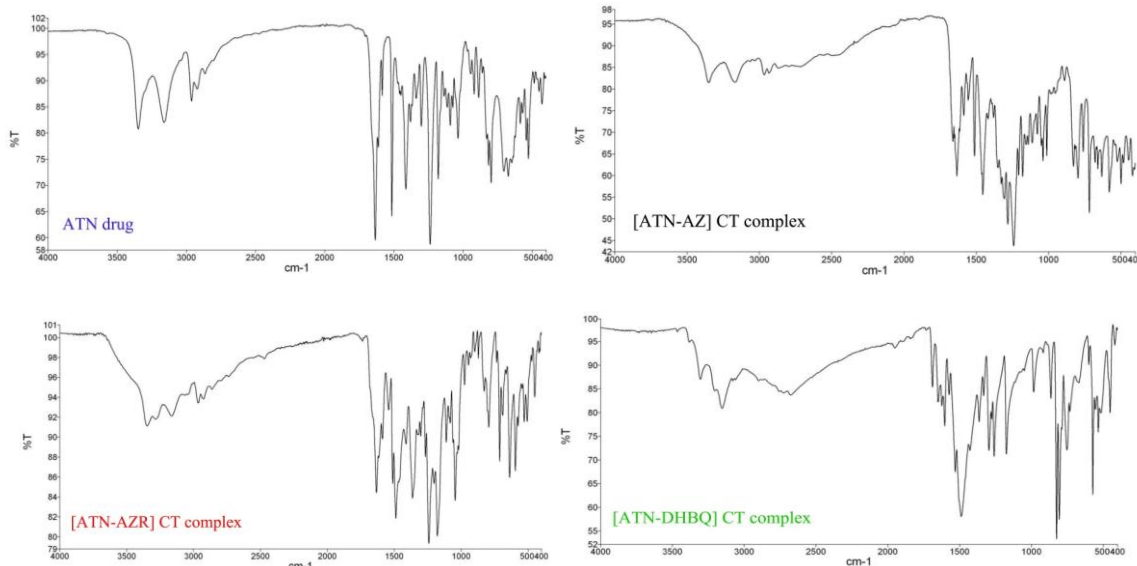
Figure 10. FTIR spectra of the ATN drug and its solid complexes in region 4000–400 cm^{-1}.

Finally, the key finding in the spectra of all ATN complexes was the broad absorption extending from 1400 to 400 cm^{-1}, which was due to the formation of H-bonds in all complexes [71]. Thus, as shown in Scheme 2, the synthesized ATN complexes exhibited high stability through CT and PT interactions.

^{1}H NMR spectra

The ^{1}H NMR spectra of ATN and its CT complexes with AZ and AZR were measured in deuterated dimethylsulfoxide (DMSO-d$_6$) (Figure 11). Signals corresponding to both ATN (i.e., the donor), and the acceptors were detected in the spectra of the complexes, mostly downfield, confirming the formation of the expected complexes. The spectrum of free ATN exhibited a broad singlet signal at 1.51 ppm, which was assigned to the NH proton. Notably, this peak was not present in the spectra of the complexes. On the other hand, sharp peaks at 2.51 and 2.63 ppm were observed in the spectra of [ATN-AZ], and [ATN-AZR] complexes, respectively. These peaks were attributed to the formation of NH$_2$$^+$ caused by the proton migration from the acceptor's hydroxyl group to the nitrogen atom of the amide moiety in ATN. Concurrently, the signals attributed to OH group in AZ or AZR [72, 73] disappeared in the spectra of the complexes, which confirmed the occurrence of a proton transfer reaction between ATN and each acceptor. Furthermore, the singlet signal of the OH moiety that appeared at 4.95 ppm in the spectrum of free ATN was not detected in the spectra of the complexes. These results were indicative of a proton transfer from the OH group of ATN to the carbonyl moiety of anthraquinone (i.e., AZ or AZR). Moreover, the signals corresponded to the aliphatic protons of (CH) and (CH$_2$) moved downfield in the spectra of the complexes as a result of H-bond formation. The signals ascribed to the aromatic protons of Az and AZR was also shifted downfield in the spectra of the complexes compared with those of free acceptors due to the π-π* transition from ATN to AZ or AZR. All of the above outcomes are consistent with the FTIR analysis and confirmed the presence of CT and PT interactions between ATN and studied acceptors.

Conclusion

Three CT complexes of ATN (i.e., electron donor) and AZ, AZR, or DHBQ (i.e., electron acceptors) were successfully prepared and comprehensively investigated in MeOH and in solid-state. New absorption bands were observed in the electronic spectra of the complexes, which confirmed the occurrence of a charge transfer reaction in a 1:1 ratio for all systems. The formation constant K_{CT} was calculated using the Benesi-Hildebrand equation, and its value was high for all ATN complexes,

demonstrating the high stability of the formed complexes in MeOH. The high stability of the ATN complexes was further confirmed from the calculated the spectrophysical parameters, the values of which were consistent with the spontaneous formation. The optical energy gap E_g of the charge transition in the investigated complexes was determined based on the electronic spectra. The values of E_g ranged from 2.02 to 2.25 eV. Furthermore, solid ATN complexes were successfully prepared and characterized, utilizing elemental analysis. Notably, the (donor: acceptor)

ratio in all complexes was found to be 1:1. The FTIR and ^{1}H NMR measurements indicated proton transfer interactions in addition to the CT interactions. Finally, simple, accurate, and sensitive spectrophotometric methods were developed to quantitatively determine the ATN in its pure form and in pharmaceutical formulations. Validation tests demonstrated that the developed methods exhibited high accurate and precise for assaying ATN without any interferences from tablet excipients.
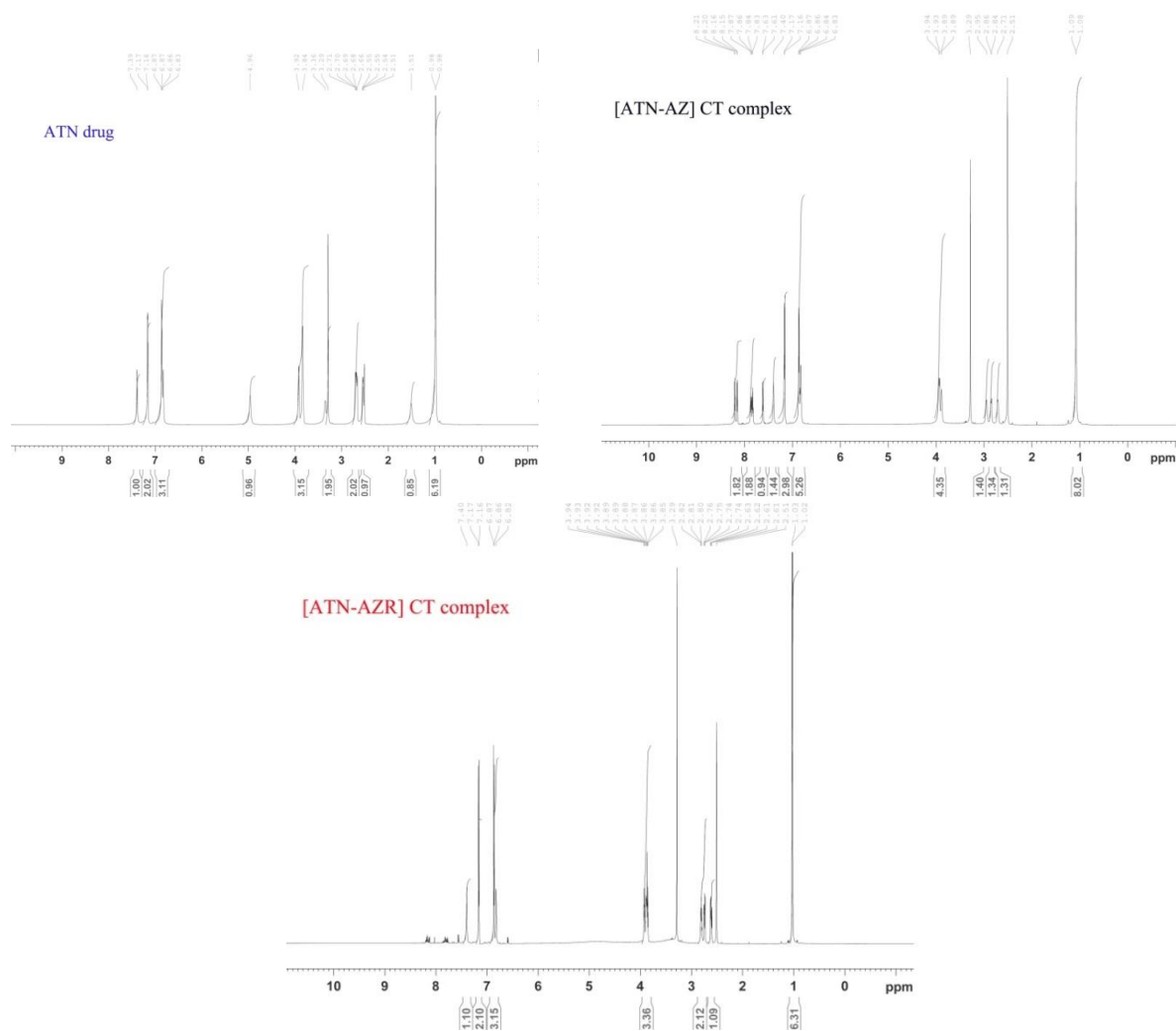

Figure 11. ^{1}H NMR spectra of the ATN drug and its solid complexes in DMSO-d6.

References

[1] Nguyen N.T. and Siegler R.W., *J Chromatography A*, **735**(1-2), 123-150(1996).

[2] Gotardo M.A., Sequinel R., Pezza L. and Pezza H.R., *Eclet. Quim.*, **33**(4), 7-14(2008).

[3] Indian Pharmacopeia, 4th ed., Ministry of Health and Family Welfare, Government of India, New Delhi (1996).

[4] Praskanth K.N. and Basavaiah K., *Acta Poloniae Pharm. Drug Res.*, **69**(2), 213-223(2012).

[5] British Pharmacopoeia, Vol. 1, London (1988).

[6] United States Pharmacopoeia, National Formulary 27, 1956-1959(2009).

[7] British Pharmacopoeia, Vol. 2, London (2001).

[8] Pyramides G., Robinson J. W. and Zito S. W., *J. Pharm. Biomed. Anal.*, **13**(2), 103-110(1995).

[9] Shafaati A. and Clark B.J., *J. Pharma. Biomed. Anal.*, **14**(11), 1547-1554(1996).

[10] Maguregui M.I., Jimenez R.M., and Alonso R. M., *J. Chromatogr. Sci.*, **36**(10), 516-522(1998).

[11] Ferraro M.C., Castellano P.M. and Kaufman, T.S. *J. Pharm. Biomed. Anal.* **34**(2), 305-314(2004).

[12] Bonato P.S. and Briguenti A.C.C., *Drug Dev. Ind. Pharm.*, **31**(2), 209 -214(2005).

[13] El-Gindy A., Emara S. and Moustafa, A., *Farmaco*, **60**, 269-280(2005).

[14] Gajewska M., Glass G. and Kostelecki J., *Acta Pol. Pharm.*, **49**, 1-10(1991).

[15] Zhao H.C., Yau N.H. and Guo J.X., *Fenxi Shiyanshi.*, **13**, 36-48(1994).

[16] Gireesh K.E., Naik M.C., Padma Y., Ramana M.V., Madhu M. and Gopinath C., *JGTPS*, **5**(3),1750–1755(2014).

[17] Sadana G.S. and Ghogare A.B., *Indian Drugs*, **28**(3), 142 -145(1990).

[18] Rao G.R., Avadhanulu A.B., Giridhar R., Pantulu A.R.R. and Kokate C.K., *East. Pharm.*, **33**(386),113-115(1990).

[19] Martinez I.R., Coque M.C.G.A. and Camanas R.M.V., *J. Chromatogr. A*, **765**(2), 221-231(1997).

[20] Argekar A.P. and Sawant J. G., *J. Liq. Chromatogr. Rel.Technol.*, **22**(10), 1571-1578(1999).

[21] Argekar A.P. and Powar S.G., *Farmaco*, **21**, 1137-1142(2000).

[22] Nikolelis D.P., Petropoulou S.E. and Mitrokotsa M.V., *Bioelectrochemistry*, **58**(1), 107-112(2002).

[23] Hassan S.S.M., Abou-Sekkina M.M., El-Ries M.A. and Wassel A.A., *J. Pharm. Biomed. Anal.*, **32**(1), 175-180(2003).

[24] Shamsipur M., Jalali F. and Haghgoo S., *Anal. Lett.*, **38**(3),401-410(2005).

[25] Goyal R.N., Gupta V.K., Oyama M. and Bachheti N., *Electrochem. Commun.*, **8**(1), 65-70(2006).

[26] Goyal R.N. and Singh S.P., *Talanta*, **69**(4), 932-937(2006).

[27] Ferraro M.C.F., Castellano P.M. and Kaufman T.S., *J. Pharm. Biomed. Anal.*, **34**(2), 305-314(2004).

[28] Bonazzi D., Gotti R., Andrisano V. and Cavrini V., *Farmaco*, **51**, 733-387(1996).

[29] Wehner W., *Die Pharmazie*, **55**(7), 543-544(2000).

[30] Ferraro M.C.F., Castellano P.M. and KaufmanT.S., *Anal. Bioanal. Chem.*, **377**(7-8), 1159-1164(2003).

[31] Agrawal Y.K., Raman K., Rajpu S. and Menon S.K., *Anal. Lett.*, **25**(8), 1503-1510(1992).

[32] Agarwal S.P., Singhal V. and Prakash A., *Indian J. Pharm. Sci.*, **60**(1), 53-55(1998).

[33] Yu L.L., Liu J.C. and Li H.K., *Yaowu Fenxi Zazhi*, **30**(3), 538-540(2010).

[34] Korang M.A., Abdel-Hay M.H., Galal S.M., Elsayed M.A., *J. Pharm. Belg.*, **40**(3), 178-184(1984).

[35] Sultan S.M., *Acta Pharm. Hung.*, **62**(6), 311-317(1992).

[36] Al-Ghannam S.M. and Belal F., *J. AOAC Int.*, **85**(4), 817-823(2002).

[37] Hiremath G.C., Mulla R.M. and Nandibewoor S.T., *Chem. Anal. (Warsaw)*, **50**, 449-455(2005).

[38] Bashir N., Shah S.W.H., Bangesh M., and Riazullah, *J. Sci. Industr. Res.*, **70**(1), 51-54(2011).

[39] Basavaiah K., Chandrashekar U., Nagegowda P., *Indian J. Chem. Technol.*, **11**(6), 769-776(2004).

[40] Issa Y.M. and Amin A.S., *Anal. Lett.*, **27**(6), 1147–1158(1994).

[41] Amin A.S., *J. Pharm. Biomed. Anal.*, **29**(4), 729–736(2002).

[42] Farhadi K., Savojbolaghi A.K. and Maleki R., *J. Chin. Chem. Soc.*, **50**(1), 153-159(2003).

[43] Shama S.A. and Amin A.S., *Spectrochim. Acta A*, **60**(8-9), 1769–1774(2004).

[44] Abdulrahman S. A. M. and Basavaiah K., *J. Saudi Chem. Soc.*, **18**(2), 107-114(2014).

[45] Hassan,W.S., El-Henawee M.M. and Gouda A.A., *Spectrochim. Acta A*, **69**(1), 245-255(2008).

[46] Kishore M., Rao Y.H. and Janardhan M., *Inter. J. Pharm. Sci. Res.*, **1**(10), 438-444(2010).

[47] Gouda A.A., El Sheikh R. and El-Azzazy R.M., *J. Anal. Bioanal. Techniques,* **3**(6), 149 (2012).

[48] Elbashir A.A. and Abdalla F.A.A., *Int. J. Pharm. Sci. Res.*, **5**(5), 22-30(2013).

[49] Alghanmi R.M., *Phys. Chem. Liq.*, **51**(3), 365–380(2013).

[50] Alghanmi R.M., *Phys. Chem. Liq.*, **51** (5), 635–650(2013).

[51] Job P., "Advanced Physicochemical Experimental", Pitman, London, UK, (1964).

[52] Benesi H.A. and Hildebrand J.H., *J. Am. Chem. Soc.*, **71**(8), 2703-2707(1949).

[53] Briegleb G., *Angew Chem.*, **76**, 326-341(1964).

[54] Aloisi G.G. and Pignataro S., *J. Chem. Soc. Faraday Trans.*, **1**, 534–539(1973).

[55] Voigt E.M. and Reid C., *J. Am. Chem. Soc.*, **86**(19), 3930–3934(1964).

[56] Rathore R., Linderman S.V. and Kochi J.K., *J. Am. Chem. Soc.*, **119**(40), 9393–9404(1997).

[57] Briegleb G. and Czekalla J., *Z. Phys. Chem. (Frankfurt)*, **24**, 37–54(1960).

[58] Person W.B., *J. Am. Chem. Soc.*, **84**(4), 536–540(1962).

[59] Alghanmi R.M. and Alhazmi L.Y., *Int. J. Pharm. Sci. Res.*, **10**(5), 2504-2515(2019).

[60] Alghanmi R.M., Soliman S.M., Basha M.T., Habeeba M.M., *J. Mol. Liq.*, **256**, 433–444(2018).

[61] Hoffman M., Martin S., Choi W. and Bahnemann D., *Chem. Rev.*, **95**(1), 69–96(1995).

[62] Mott N.F. and Davis E.A., "Electronic Process in Non-crystalline Materials", Calendron Press, Oxford (1972).

[63] Fu M.L., Guo G.C., Liu X., Cai L.Z. and Huang J.S., *Inorg. Chem. Commun.*, **8**, 18–21(2005).

[64] Adam A.M.A., Refat M.S., Hegab M.S. and Saad H.A., *J. Mol. Liq.*, **224**(part A), 311–321(2016).

[65] International Conference on Harmonization of Technical Requirements for Registration of Pharmaceuticals for Human Use. ICH Harmonized Tripartite Guideline, Validation of Analytical Procedures: Text and Methodology, Q2(R1). Complementary Guideline on Methodology dated 06 November 1996, ICH, London 2005.

[66] Esteves de Castro R.A., Canotilho J., Barbosa R.M., Ramos Silva M., MatosBeja A., Paixao J.A., and Redinha J.S., *Cryst. Growth Des.*, **7**(3), 496-500(2007).

[67] Cozar O., Szabo L., Cozar I.B., Leopold N., David L., CaØinap C. and Chis V., *J. Mol. Struct.*, , **993**(1-3), 357-366(2011).

[68] ElHabeeb A.A., *Orient. J. Chem.*, **30**(4), 1441-1462(2014).

[69] Ranjitha S., Aroulmoji V., Mohrb T., Anbarasand P.M., and Rajarajane G., *ACTA PHYSICA POLONICA A*, **126**, 833-839(2014).

[70] Ortiz E., Solis H., Noreña L. and Loera-Serna S., *International Journal of Environmental Science and Development*, **8**(4), 255-259(2017).

[71] Alghanmi R.M., *J. Chem.*, **2019**, 14 pages (2019).

[72] Doskocz M., Kubas K., Frackowiak A. and Gancarz R., *Polyhedron*, **28**(11), 2201-2205(2009).

[73] Chin Y.P., Abdul Raof S.F., Sinniah S., Lee V.S., Mohamad S. and Abdul Manan N.S., *J. Mol. Struct.*, **1083**, 236-244(2015).